
Reconstruct the Pruned Model without Any Retraining

Pingjie Wang, Ziqing Fan, Shengchao Hu, Zhe Chen
Yanfeng Wang, Yu Wang*

Shanghai Jiao Tong University

Shanghai Artificial Intelligence Laboratory

{pingjiawang, zqfan_knight, charles-hu, chenzhe2018}@sjtu.edu.cn

{wangyanfeng622, yuwangsjtu}@sjtu.edu.cn

Abstract

Structured pruning is a promising hardware-friendly compression technique for large language models (LLMs), which is expected to be retraining-free to avoid the enormous retraining cost. This retraining-free paradigm involves (i) *pruning criteria* to define the architecture and (ii) *distortion reconstruction* to restore performance. However, existing methods often emphasize pruning criteria while using reconstruction techniques that are specific to certain modules or criteria, resulting in limited generalizability. To address this, we introduce the **Linear Interpolation-based Adaptive Reconstruction (LIAR)** framework, which is both efficient and effective. LIAR does not require back-propagation or retraining and is compatible with various pruning criteria and modules. By applying linear interpolation to the preserved weights, LIAR minimizes reconstruction error and effectively reconstructs the pruned output. Our evaluations on benchmarks such as GLUE, SQuAD, WikiText, and common sense reasoning show that LIAR enables a BERT model to maintain 98% accuracy even after removing 50% of its parameters and achieves top performance for LLaMA in just a few minutes.

1 Introduction

Large language models (LLMs) have attained significant achievements towards various downstream tasks in recent years [1, 2, 3, 4]. However, despite the substantial progress, the deployment of LLMs is constrained by the high parameter counts and considerable computational overhead [5]. Retraining-based structured pruning [6, 7] is one of the compression techniques to address this issue. By removing a whole group of weights from the original model, such methods can reduce the inference latency and memory storage without requiring any external hardware acceleration support [8]. However, such a strategy requires a full dataset to retrain the pruned model, resulting in significant computational overhead (e.g. ~ 33 hours for BERT [6]) and extensive engineering efforts for hyper-parameter tuning and complex deployment [9, 10]. These requirements render the approach impractical for real-world applications, especially for LLMs.

The Retraining-free pruning paradigm is proposed to reduce the enormous retraining consumption, which falls into two stages: 1) *pruning criteria* and 2) *distortion reconstruction*. For the first stage, each module of the well-trained model is scored based on a specific criterion to identify and prune redundant components [11, 12]. After that, the distorted output is reconstructed by the subsequent reconstruction stage. Compared to retraining-based approaches, the unique value of such a paradigm is its ability to regain performance without any training and only requires a small calibration dataset. Consequently, it is highly efficient (e.g., several minutes) and well-suited for compressing LLMs.

*Corresponding author.

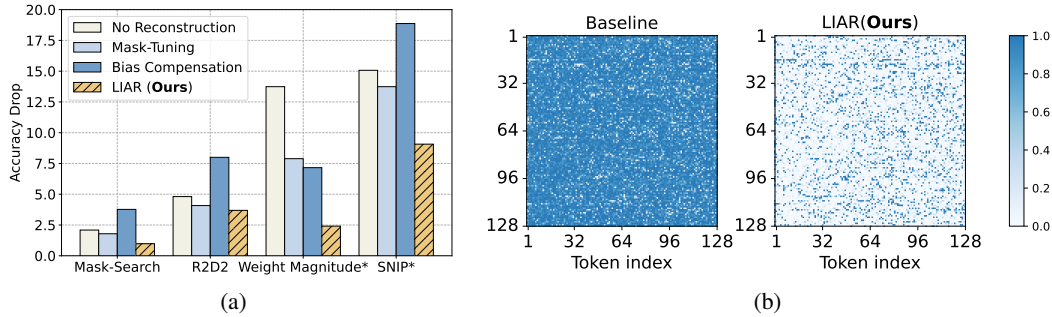


Figure 1: (a) Accuracy drop on the STS-B task by dropping 70% FFN neurons of BERT with various pruning criteria (*x-axis*) and reconstruction methods (*legends*). ‘*’ means the retraining-based criteria. (b) Reconstruction error across different tokens and samples by Bias Compensation and LIAR.

However, there is limited research about retraining-free approaches, and most previous works target either encoder-based or decoder-based models exclusively. Additionally, existing retraining-free methods primarily focus on developing better criteria for determining the pruned architecture, with proposed reconstruction techniques often lacking generalizability. As illustrated in Figure 1a, we applied different algorithms [13, 14] to reconstruct models pruned using manifold criteria [13, 15, 16, 17] and compared the accuracy drop. Our results reveal that existing reconstruction approaches exhibit limited and unstable performance, particularly for retraining-based criteria. Therefore, despite the efficiency of the retraining-free pruning paradigm, its applicability remains significantly restricted.

To tackle this challenge, we introduce a **Linear Interpolation-based Adaptive Recovery (LIAR)** framework, an efficient and effective distortion reconstruction framework for retraining-free structured pruning. In this framework, we reformulate the reconstruction problem as the estimation of the pruned output, and utilize the reserved modules to approximate the pruned ones, which achieves a much lower reconstruction error than the existing work as shown in Figure 1b. Through this framework, our reconstruction algorithm can not only be applied to both encoder- and decoder-based models, but also generalize better on extensive pruning criteria that are not originally designed for such a retraining-free paradigm, which is exhibited in Figure 1a. In this way, it largely boosts the application potential for efficient model compression.

To evaluate the compression performance enhancement capability of our LIAR framework, we conduct experiments on both BERT_{BASE} and LLaMA models family for GLUE, SQuAD, WikiText, 7 common sense reasoning benchmarks for sequence classification, question answering (QA), language modeling and zero-shot performance validation respectively. We also assess the performance of LIAR for different modules and pruning criteria to investigate the generalizability of our reconstruction framework. Our contributions can be summarized as follows:

- **Framework.** We reformulate the distortion reconstruction problem, and propose LIAR, an efficient, effective, and unsupervised reconstruction framework that requires no backward propagation or retraining. It utilizes the preserved modules to approximate the impacts of the pruned ones, thereby achieving efficient and accurate performance reconstruction.
- **Performance.** We show that LIAR achieves the highest accuracy compared with existing state-of-the-art (SOTA) retraining-free pruning approaches on both BERT_{BASE} and LLaMA family models on 4 categorized benchmarks. Notably, LIAR achieves 98% accuracy for BERT_{BASE} with 50% parameters pruned.
- **Generalization.** We conduct extensive experiments to verify that LIAR is capable of generalizing across different modules and criteria. This increases the utility of both retraining-based and retraining-free criteria within the retraining-free paradigm, thereby expanding their range of applications.

Table 1: Comparison between various reconstruction methods for PLMs concerning different aspects. ✓ and ✗ represent whether the method had the specific feature or not.

Reconstruction Method	Encoder-based Models	Decoder-based Models	High Pruning Ratio	Arbitrary Pruning Criteria
No reconstruction	✗	✗	✗	✗
Mask-Tuning [13, 15]	✓	✗	✗	✓
Bias Compensation [14]	✗	✓	✗	✗
LIAR (Ours)	✓	✓	✓	✓

2 Related Works

2.1 Network Pruning for Language Models

Network pruning is a widely applicable compression technique, whose key point is to remove the redundant weight or modules from the original network [18] and reserve the salient ones [11, 12]. It is broadly categorized from the granularity aspect into structured and unstructured pruning. Unstructured pruning [19, 20, 21] performs at the individual weight level, which brings about larger sparsity but fails to accelerate the model and reduce the storage cost without requiring additional hardware support. By contrast, structured pruning [22, 23, 24] removes a group of weights, such as an entire channel, head, layer, and so on, therefore providing a more hardware-friendly solution, enhancing the lower inference latency and memory demands, so we focus on structured pruning in this paper.

The conventional retraining-based paradigm involves compressing the original model using various criteria followed by retraining to restore performance [25, 26, 27, 28]. However, as the size and complexity of LLMs rapidly increase [29, 30, 31], this conventional approach becomes impractical and costly, prompting the need for retraining-free compression techniques. Recent developments in this area have primarily centered around quantization [32, 33, 34] and have expanded to include pruning methods [13, 15, 14] that eliminate the need for retraining. In this paper, our work targets enhancing the performance of the retraining-free pruning paradigm, which can reduce the model size, lower the memory consumption, accelerate the inference, and be orthogonal and compatible with quantization for further compression simultaneously.

2.2 Distortion Reconstruction for Retraining-free Pruning

In the context of network pruning, retraining-free approaches such as those proposed by [35] seek to mitigate output distortion instead of retraining to maintain as much of the model’s original capability as possible. Mask-Tuning, introduced by [13] and adopted by KCM [15], involves rescaling the mask as a reconstruction technique. While it tests the limits of encoder-based models, it struggles to maintain performance at high pruning ratios. FLAP [14] introduced a bias compensation method to correct the distorted output of pruned layers. However, it is tailored to its specific pruning metric and may not broadly apply to other effective pruning criteria, sometimes leading to unstable performance as discussed in Figure 1a. Our proposed framework overcomes these limitations by significantly narrowing the performance gap between the original and pruned models, especially at higher pruning ratios, and maintains stable effectiveness across various pruning standards as detailed in Table 1.

3 Preliminaries

Post-training pruning. Given a computational constraint and a sampled calibration dataset, the target of post-training pruning is to prune a well-optimized model to satisfy the constraint. Considering a fine-tuned model \mathcal{M} and a constraint \mathcal{C} , optimal structured pruning is usually defined with respect to minimizing the accuracy loss:

$$\arg \min_{\mathcal{M}} \mathcal{L}(\mathcal{M}) \quad s.t. \quad Cost(\mathcal{M}) \leq \mathcal{C}, \quad (1)$$

where $Cost(\cdot)$ is a calculation function of computational complexity. In the retraining-free context, $\mathcal{L}(\mathcal{M})$ can also be replaced with feature map loss or other metrics [14, 15].

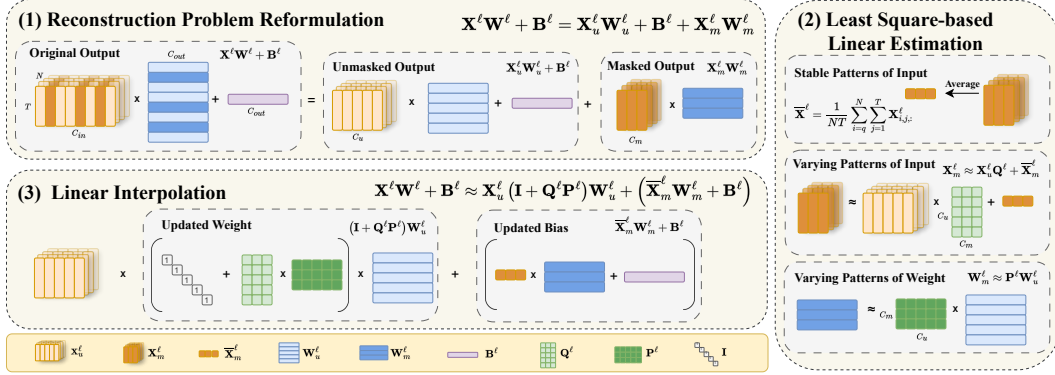


Figure 2: Overview of LIAR framework. The original output is first reformulated by **(1) Reconstruction Problem Reformulation**, and then the masked output is estimated by **(2) Least Square-based Linear Estimation**. Finally, the model weight and bias are updated with **(3) Linear Interpolation**.

Layer-wise Pruning. For post-training pruning, globally solving the pruning problem is challenging and technically infeasible due to the enormous neural architecture search expense. A practical solution for it is to split the full-model problem into layer-wise subproblems as [21] demonstrated. Given an input \mathbf{X}^ℓ of shape (N, T, C_{in}) with N instances and sequence length T for layer ℓ , a weight \mathbf{W}^ℓ of shape (C_{in}, C_{out}) and bias \mathbf{B}^ℓ of shape $(C_{out},)$, the quality of the layer-wise solution for structured pruning is usually measured by the ℓ_2 -error between the original output and the pruned output as

$$\mathbf{M}^\ell, \widehat{\mathbf{W}}^\ell = \arg \min_{\mathbf{M}^\ell, \widehat{\mathbf{W}}^\ell} \left\| \mathbf{X}^\ell \mathbf{W}^\ell + \mathbf{B}^\ell - \mathbf{X}^\ell (\mathbf{M}^\ell \odot \widehat{\mathbf{W}}^\ell) - \widehat{\mathbf{B}}^\ell \right\|_2^2, \quad (2)$$

where $\mathbf{M}^\ell \in \mathbb{R}^{C_{in}}$ denotes the mask vector of layer ℓ , $\|\cdot\|_2^2$ denotes the ℓ_2 -error, $\widehat{\mathbf{W}}^\ell$ and $\widehat{\mathbf{B}}^\ell$ are the weight and bias of the pruned model and probably updated from \mathbf{W}^ℓ and \mathbf{B}^ℓ through retraining.

4 LIAR: Linear Interpolation-based Adaptive Recover

4.1 Motivation

To conduct a more detailed analysis of the reconstruction problem, we would like to first reformulate the pruning and reconstruction process. Considering a transformation function with weight \mathbf{W}^ℓ and bias \mathbf{B}^ℓ , we reformulate the original output $\mathbf{X}^\ell \mathbf{W}^\ell + \mathbf{B}^\ell$ to investigate how the counterparts derive the output and result in the distortion after pruning:

$$\mathbf{X}^\ell \mathbf{W}^\ell + \mathbf{B}^\ell = \underbrace{\mathbf{X}_u^\ell \mathbf{W}_u^\ell + \mathbf{B}^\ell}_{\text{unmasked output}} + \underbrace{\mathbf{X}_m^\ell \mathbf{W}_m^\ell}_{\text{masked output}}, \quad (3)$$

where \mathbf{X}_u^ℓ of shape (N, T, C_u) and \mathbf{W}_u^ℓ of shape (C_u, C_{out}) denote the unmasked input activation and weight. By contrast, the product of the masked input \mathbf{X}_m^ℓ of shape (N, T, C_m) and weight \mathbf{W}_m^ℓ of shape (C_m, C_{out}) , leads to the output distortion and performance degradation if pruned directly, and it is also the retraining or reconstruction target to guarantee the output fidelity.

In the circumstance of the conventional pruning, the masked output is regained by retraining the unmasked weight \mathbf{W}_u^ℓ and bias \mathbf{B}^ℓ , while we target resolving this problem by approximating the masked component with the unmasked output. The reconstruction error of k -th channel of layer ℓ is defined as

$$\varepsilon_k^\ell = \frac{\|\widehat{\mathbf{X}}_{\cdot, \cdot, k}^\ell - \mathbf{X}_{\cdot, \cdot, k}^\ell\|_2^2}{\|\mathbf{X}_{\cdot, \cdot, k}^\ell\|_2^2}, \quad (4)$$

and a lower reconstruction error typically indicates better performance retention.

Previous work [14] approximated the pruned output by utilizing the stability of part of the channels, which exhibit fairly stable patterns given different samples and thus can be compensated with a bias

term. The reconstructed representation for channel k is the averaged value, which is formulated as $\bar{\mathbf{X}}_k^\ell = \frac{1}{NT} \sum_{i=1}^N \sum_{j=1}^T \mathbf{X}_{i,j,k}^\ell$. Such a stability-based approach may work for some stable channels, but fails to reconstruct the ones with high fluctuations as demonstrated in Figure 1b (left part).

4.2 Method

To address the issue of instability in certain channels, we propose to approximate the varying patterns that cannot be compensated by the averaged value. Specifically, we reconstruct the varying patterns of pruned channel k with a linear combination of the others, which is formulated as $\hat{\mathbf{X}}_{::,k}^\ell = \bar{\mathbf{X}}_k^\ell + \sum_{l=1, l \neq k}^{C_{in}} m_l \mathbf{X}_{::,l}^\ell$, where $m_l \in \mathbb{R}$ is a scalar that determines the contribution of channel l to reconstruct the channel k . It is calculated by the least square algorithm. As shown in Figure 1b (right part), compared to the stability-based one, our method achieves much lower reconstruction error.

Furthermore, we introduce our **Linear Interpolation-based Adaptive Reconstruction (LIAR)** framework. This method approximates the pruned \mathbf{X}_m^ℓ and \mathbf{W}_m^ℓ using the remaining \mathbf{X}_u^ℓ and \mathbf{W}_u^ℓ . We compute the transformation matrices and apply linear interpolation to the preserved weight matrix \mathbf{W}_u^ℓ to effectively reconstruct the distortion introduced by pruning.

To be specific, we first define a transformation matrix \mathbf{Q}^ℓ to approximate the varying patterns of \mathbf{X}_m^ℓ by \mathbf{X}_u^ℓ as

$$\mathbf{X}_m^\ell \approx \mathbf{X}_u^\ell \mathbf{Q}^\ell + \bar{\mathbf{X}}_m^\ell, \quad (5)$$

where $\mathbf{Q}^\ell \in \mathbb{R}^{C_u \times C_m}$ is derived by the least square algorithm to minimize the reconstruction error:

$$\mathbf{Q}^\ell = \arg \min_{\mathbf{Q}^\ell} \left\| \mathbf{X}_m^\ell - \left(\mathbf{X}_u^\ell \mathbf{Q}^\ell + \bar{\mathbf{X}}_m^\ell \right) \right\|_2^2. \quad (6)$$

The masked weight matrix \mathbf{W}_m^ℓ can be reconstructed following a similar procedure:

$$\mathbf{W}_m^\ell \approx \mathbf{P}^\ell \mathbf{W}_u^\ell, \quad (7)$$

where $\mathbf{P}^\ell \in \mathbb{R}^{C_m \times C_u}$ is determined in the same way as Equation (6). We do not include a bias term as in Equation (5) because stability was not observed for the weight matrices.

Having successfully reconstructed \mathbf{X}_m^ℓ and \mathbf{W}_m^ℓ , we can now seamlessly combine them to achieve a distortion-free output. Consequently, $\mathbf{X}_m^\ell \mathbf{W}_m^\ell$ is redefined as:

$$\begin{aligned} \mathbf{X}_m^\ell \mathbf{W}_m^\ell &\approx (\mathbf{X}_u^\ell \mathbf{Q}^\ell + \bar{\mathbf{X}}_m^\ell) \mathbf{W}_m^\ell \\ &= \mathbf{X}_u^\ell \mathbf{Q}^\ell \mathbf{W}_m^\ell + \bar{\mathbf{X}}_m^\ell \mathbf{W}_m^\ell \\ &= \mathbf{X}_u^\ell \mathbf{Q}^\ell \mathbf{P}^\ell \mathbf{W}_u^\ell + \bar{\mathbf{X}}_m^\ell \mathbf{W}_m^\ell. \end{aligned} \quad (8)$$

Then we substitute Equation (8) to (3) and obtain

$$\begin{aligned} \mathbf{X}^\ell \mathbf{W}^\ell + \mathbf{B}^\ell &\approx \mathbf{X}_u^\ell \mathbf{W}_u^\ell + \mathbf{B}^\ell + \mathbf{X}_u^\ell \mathbf{Q}^\ell \mathbf{P}^\ell \mathbf{W}_u^\ell + \bar{\mathbf{X}}_m^\ell \mathbf{W}_m^\ell \\ &= \mathbf{X}_u^\ell \left(\mathbf{I} + \mathbf{Q}^\ell \mathbf{P}^\ell \right) \mathbf{W}_u^\ell + \left(\bar{\mathbf{X}}_m^\ell \mathbf{W}_m^\ell + \mathbf{B}^\ell \right), \end{aligned} \quad (9)$$

where \mathbf{I} of shape (C_u, C_u) is the identity matrix, the preserved weight \mathbf{W}_u^ℓ and bias \mathbf{B}^ℓ are updated to $(\mathbf{I} + \mathbf{Q}^\ell \mathbf{P}^\ell) \mathbf{W}_u^\ell$ and $(\bar{\mathbf{X}}_m^\ell \mathbf{W}_m^\ell + \mathbf{B}^\ell)$, respectively. By Interpolating the transformation matrices to the preserved weights and bias, we achieve to reconstruct the output distorted by direct pruning.

4.3 Framework

We visualize our framework in Figure 2, which includes (1) Reconstruction Problem Reformulation, (2) Least-Square-based Linear Estimation, and (3) Linear Interpolation. Specifically, considering a function with weight \mathbf{W}^ℓ and bias \mathbf{B}^ℓ , we first reformulate the original output and split it into the masked and unmasked ones, denoted as $\mathbf{X}_m^\ell \mathbf{W}_m^\ell$ and $\mathbf{X}_u^\ell \mathbf{W}_u^\ell + \mathbf{B}^\ell$. Secondly, we estimate the stable and varying patterns of the masked input \mathbf{X}_m^ℓ and weight \mathbf{W}_m^ℓ and obtain the transformation matrices \mathbf{Q}^ℓ and \mathbf{P}^ℓ by the least square algorithm. Finally, with the obtained transformation matrices, we apply linear interpolation to the preserved weight and bias to reconstruct the pruned output. The comprehensive details of our method are further described in Appendix A.

Table 2: Sequence classification and QA performance of the pruned BERT_{BASE} on the GLUE benchmark and SQuAD datasets. “Naive” represents the results without retraining and reconstruction.

Ratio	Criterion	Reconstruction	MNLI \uparrow	MRPC \uparrow	STS-B \uparrow	SST-2 \uparrow	QNLI \uparrow	QQP \uparrow	SQuAD _{1.1} \uparrow	SQuAD _{2.0} \uparrow	Average \uparrow
Dense	-	-	84.53	86.27	88.59	93.12	91.41	91.00	88.48	76.82	87.53
30%	KCM	Naive	75.87	66.91	86.65	91.28	84.53	87.23	75.62	38.70	75.85
		KCM	80.49	85.54	86.51	92.09	88.12	89.41	84.62	72.66	84.93
		LIAR	82.90	84.31	87.54	92.20	89.09	90.16	86.13	72.90	85.65
	Mask-Tuning	Naive	83.63	84.31	88.34	92.78	90.23	90.75	87.08	75.49	86.58
		Mask-Tuning	83.05	86.76	88.38	92.66	90.79	90.72	87.55	76.06	87.00
		LIAR	84.10	86.52	88.63	93.00	91.01	90.85	87.91	75.56	87.20
50%	KCM	Naive	50.20	34.31	82.63	64.11	79.33	73.59	47.63	24.23	57.00
		KCM	50.20	34.31	82.63	64.11	79.33	73.59	48.99	24.23	57.17
		LIAR	76.36	78.92	83.65	90.25	80.91	87.98	76.36	53.10	78.44
	Mask-Tuning	Naive	76.67	81.37	86.81	89.33	87.00	88.69	77.18	56.70	80.47
		Mask-Tuning	80.87	83.58	86.92	91.74	88.94	89.53	81.67	68.26	83.94
		LIAR	82.87	86.27	87.92	92.43	88.76	90.17	85.45	71.81	85.71

5 Experiments

5.1 Experimental Setup

Models. We conduct experiments on two representative and widely used models with different architectures and sizes: BERT_{BASE} [36] (0.1B) and LLaMA family models [37] (7B, 13B and 30B), which are encoder- and decoder-based respectively.

Tasks. To verify the widespread adoption of our proposed framework, we evaluate LIAR on four categories of capabilities: the sequence classification performance on the GLUE benchmark [38], the question-answering capability on SQuAD_{1.1} [39] and SQuAD_{2.0} [40] datasets, the language modeling capability on the WikiText-2 [41] dataset, and the zero-shot performance across seven common sense reasoning tasks [42, 43, 44, 45, 46, 47].

Baselines. To validate the effectiveness of our reconstruction algorithm, we compare the performance reconstructed with various state-of-the-art structured pruning approaches. These include retraining-based method like LLM-Pruner [48], and retraining-free algorithms, such as Mask-Tuning [13], KCM [15], and FLAP [14]. The baseline reconstruction methods include Mask-Tuning [13] and Bias Compensation [14].

Pruning Criteria & Reconstruction. Finally, to evaluate the generalization ability to various pruning criteria across different pruning ratios, we test LIAR with two representative retraining-based pruning metrics: Weight Magnitude [16] and SNIP [17]. These metrics use the magnitude and the first derivative of the model weight respectively, and are known as zero- and first-order criteria.

Implementation Details. We implement the framework using the Pytorch [49] and Huggingface Transformers library [50]. Specifically, the least square algorithm is implemented by the linear solver² to derive the solution for Equation (6). All the experiments for both the BERT_{BASE} and LLaMA models are conducted on one single NVIDIA Tesla A100 80G GPU. Please see Appendix B and C for more experimental settings and implementation details.

5.2 Classification & QA Tasks Performance

We first establish the classification and QA performance on the GLUE and SQuAD benchmarks for the encoder-based BERT_{BASE} model with SOTA retraining-free methods: Mask-Tuning [13] and KCM [15]. To be specific, we only adopt their pruning criteria and compare the performance recovered by LIAR with naive pruning (no reconstruction) and baselines.

As shown in Table 2, the performance with LIAR significantly and consistently outperforms both baselines. Notably, it retains 99.6% accuracy even after removing 20% of encoder parameters. It also prunes 50% of parameters with only a 2% performance degradation compared to the uncompressed BERT_{BASE}, without any retraining. Furthermore, LIAR greatly enhances the performance derived

²torch.linalg.lstsq

Table 3: Perplexity of the pruned LLaMA-7B, LLaMA-13B and LLaMA-30B on the WikiText.

Ratio	Criterion	Reconstruction	7B↓	13B↓	30B↓	Pruning ratio	Criterion	Reconstruction	7B↓	13B↓	30B↓
Dense	-	-	12.62	10.81	9.11	Dense	-	-	12.62	10.81	9.11
20%	LLM-Pruner	Naive	19.28	16.59	12.35	50%	LLM-Pruner	Naive	112.44	76.40	36.16
		FLAP	18.15	15.92	11.97			FLAP	82.60	44.82	26.66
		LIAR	15.92	13.75	11.67			LIAR	43.96	30.15	19.58
	FLAP	Naive	16.15	14.75	11.96		FLAP	Naive	52.74	36.37	26.11
		FLAP	14.62	14.17	11.46			FLAP	31.80	24.83	20.54
		LIAR	14.07	12.71	10.93			LIAR	25.43	21.11	16.93

Table 4: Zero-shot task accuracy of the pruned LLaMA-7B on common sense reasoning benchmarks.

ratio	Criterion	Reconstruction	ARC-c↑	ARC-e↑	BoolQ↑	HellaSwag↑	OBQA↑	PIQA↑	WinoGrande↑	Average↑
Dense	-	-	44.71	72.85	75.02	76.20	44.40	79.16	70.01	66.05
20%	LLM-Pruner	Naive	38.14	63.30	57.58	69.13	39.80	75.35	63.77	58.15
		FLAP	36.77	65.53	61.93	68.53	41.40	75.73	63.61	59.07
		LIAR	39.08	65.24	66.64	67.62	41.80	76.61	64.64	60.23
	FLAP	Naive	38.05	64.18	52.63	71.12	40.60	77.04	68.82	58.92
		FLAP	38.05	65.32	56.94	71.18	39.40	76.82	68.27	59.43
		LIAR	40.61	68.52	74.37	70.00	42.40	77.69	67.01	62.94
50%	LLM-Pruner	Naive	25.77	34.81	46.94	36.14	30.20	60.55	53.12	41.08
		FLAP	26.88	36.49	42.75	37.64	32.00	62.62	52.49	41.55
		LIAR	26.79	43.31	56.73	39.56	31.60	63.98	52.17	44.88
	FLAP	Naive	29.95	45.83	59.48	52.96	36.60	67.90	57.93	50.09
		FLAP	29.27	47.22	59.63	52.13	34.60	67.52	57.06	49.63
		LIAR	33.96	55.89	62.51	50.51	35.60	67.68	60.22	52.34

by naive pruning without recovery. For instance, it improves performance by 37.6% for KCM at a 50% pruning ratio.

5.3 Language Modeling & Zero-shot Tasks Performance

Moreover, to assess the general applicability of LIAR, we conduct tests on the decoder-based LLaMA family models. Specifically, we apply LIAR to the SOTA approaches for LLMs: LLM-Pruner [48] and FLAP [14]. It is noted that as LLM-Pruner is retraining-based, we here adopt the reconstruction method of FLAP to recover its performance as a baseline.

Table 3 demonstrates that LIAR acts as a significant reconstruction framework on the language modeling task, especially at a high pruning ratio. For example, compared to naive pruning, LIAR enhances the performance by $2.56\times$ and $2.07\times$ for the LLaMA-7B model with 50% parameters pruned by LLM-Pruner and FLAP respectively. For zero-shot common sense reasoning tasks, LIAR also enhances the performance of the pruned models on most tasks as shown in Table 4.

5.4 Generalization Ability Evaluation

We also compare the generalization ability of our reconstruction framework with existing approaches. Specifically, we validate the generalization ability with different pruning modules and criteria across diverse especially high pruning ratios. Here we adopt Naive pruning, Bias Compensation [14], and Mask-Tuning [13] as baselines, in which naive pruning signifies no reconstruction.

Generalization to Pruning Modules. To assess the reconstruction capability of our framework on different modules, we apply LIAR to reconstruct attention heads and FFN hidden channels, which we refer to as the FFN neurons. Specifically, we first utilize the pruning criterion of [13] to prune only heads or neurons of BERT_{BASE}, then we apply different reconstruction algorithms to regain the performance, while the remaining elements stay frozen.

Figure 3 depicts that Bias Compensation leads to somewhat unstable performance, especially in the STS-B and QQP tasks, where it often results in lower accuracy than naive pruning. This decrease in accuracy might stem from substantial variations in the hidden states across certain tasks and the failure of the estimated bias to restore the altered outputs. In contrast, LIAR and Mask-Tuning show more stable improvements in recovery. Particularly, LIAR consistently enhances accuracy, markedly when a significant proportion of heads or neurons are pruned, such as 30% and 10%.

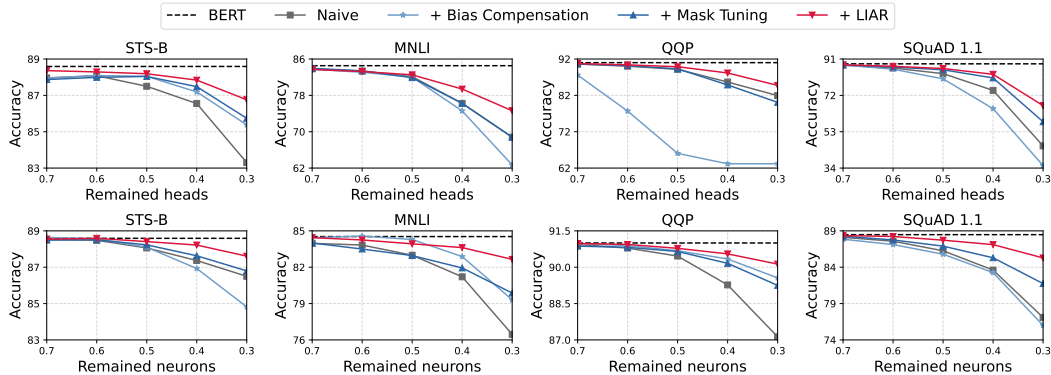


Figure 3: Accuracy comparison of $BERT_{BASE}$ on STS-B, MNLI, QQP and SQuAD_{1.1} tasks by pruning attention heads (**upper**) and FFN neurons (**lower**) with different reconstruction strategies.

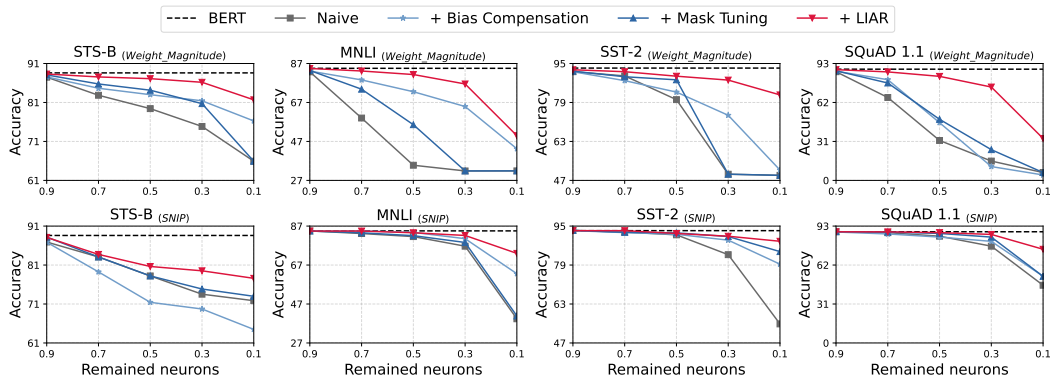


Figure 4: Accuracy comparison of the $BERT_{BASE}$ pruned by Weight Magnitude-based (**upper**) and SNIP (**lower**) criteria on the STS-B, MNLI, SST-2 and SQuAD_{1.1} tasks respectively. We only prune the FFN neurons to avoid introducing the architecture search problem.

Generalization to Pruning Criteria. Finally, to verify the generalization ability to manifold pruning algorithms, we apply LIAR on two retraining-based pruning criteria: Weight Magnitude [16] and SNIP [17], which are zero-order and first-order respectively.

Figure 4 shows that LIAR significantly improves performance under all pruning ratios compared to simple pruning without any reconstruction. Furthermore, LIAR reduces the gap between different pruning metrics, for instance, on the SST-2 task. Interestingly, the STS-B accuracy derived from the Weight Magnitude-based criterion with 90% neurons pruned outperforms SNIP after being reconstructed by LIAR, even though it performs worse without reconstruction. This likely indicates that less effective pruning metrics can have higher recoverability. More results about the generalization performance on other tasks are demonstrated in Appendix C.7 and C.8.

5.5 Ablation Study

In this subsection, we will present additional visualizations of the reconstruction error throughout the entire model, analyze the effectiveness of updates to the weight and bias terms in LIAR, evaluate the robustness of LIAR with respect to calibration samples, and assess the time consumption involved.

Reconstruction Error. While Figure 1b only depicted the reconstruction error for a single channel, we now present a more comprehensive analysis of the error distribution across the entire model. As demonstrated in Figure 5a, LIAR significantly reduces the error in reconstructing the model’s output.

Interpolated Weight & Bias. As mentioned earlier, we reconstruct the distorted output by integrating and updating a weight and bias term into the original matrices. To evaluate their significance, we

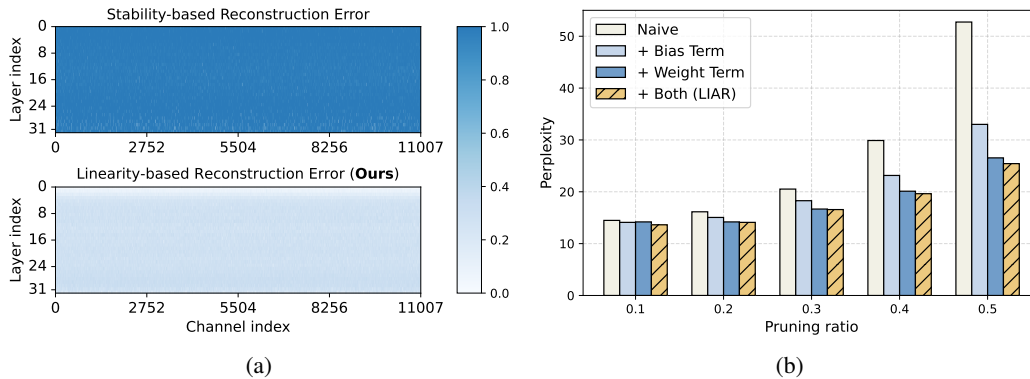


Figure 5: (a) Reconstruction error distribution of the hidden input of LLaMA-7B across 1024 instances sampled from the WikiText-2 training dataset. (b) Perplexity comparison of the LLaMA-7B by removing the updation for the bias and weight term at various pruning ratios.

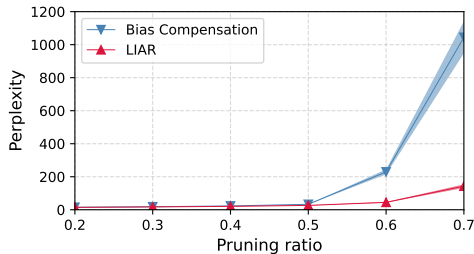


Figure 6: Dynamic perplexity range of LLaMA-7B on WikiText, which is fed with 128, 256, 512, and 1024 samples respectively.

Table 5: Time consumption (minutes) for reconstructing LLaMA models with different numbers of calibration samples. We conduct the experiments on one single NVIDIA Tesla A100 80G GPU.

Model	Calibration Samples			
	128	256	512	1024
LLaMA-7B	1.0	1.5	2.1	3.9
LLaMA-13B	3.1	3.8	4.9	7.9
LLaMA-30B	6.6	8.5	12.7	19.7

modify Equation (9) by retaining the update for either the weight or the bias term, while omitting the other. The perplexity of the LLaMA-7B model, as illustrated in Figure 5b, demonstrates that both the weight and bias updates are vital for reconstructing the pruned components, with the weight term playing a more significant role.

Robustness to Calibration Samples. Since we utilize a calibration dataset to assist in estimating the weight and bias terms of Equations (5)-(7), we also evaluate the impact of the size of this dataset to ensure the usability under low-resource conditions. Specifically, we prune the LLaMA-7B model using FLAP, and apply Bias Compensation and LIAR to reconstruct it respectively. As shown in Figure 6, LIAR consistently maintains a low dynamic perplexity range, consistently outperforming FLAP as the pruning ratio varies from 0.2 to 0.7. This indicates that our method is highly efficient, requiring only a few or even a single forward propagation, without the need for back-propagation.

Time Consumption. To further analyze the efficiency of our approach, we record the time consumption for LLaMA models using varying numbers of calibration samples. Table 5 shows that the time required increases with both model size and the number of samples. Notably, LIAR consistently demonstrates low time costs on larger models, particularly completing tasks with the LLaMA-7B model in just under one minute. It’s important to highlight that LIAR was tested using a single GPU in these experiments, suggesting that its efficiency could improve even further with additional computational resources.

6 Conclusion

In this paper, we propose LIAR (**L**inear **I**nterpolation-based **A**daptive **R**econstruction), an efficient and effective reconstruction framework with no need for back-propagation and retraining and compatible with various pruning modules and criteria. LIAR leverages the preserved modules to approximate the

masked ones, reconstructing the output distortion by applying linear interpolation to the preserved weight matrix. We empirically evaluate the validity of LIAR on GLUE, SQuAD, WikiText-2, and common sense reasoning benchmarks respectively, where the method with LIAR reduces 50% encoder parameters within only 2% accuracy degradation for BERT_{BASE}, and achieves 2.56× performance enhancement for LLaMA-7B under the 50% pruning ratio within 1 minute.

References

- [1] Aohan Zeng, Xiao Liu, Zhengxiao Du, Zihan Wang, Hanyu Lai, Ming Ding, Zhuoyi Yang, Yifan Xu, Wendi Zheng, Xiao Xia, et al. Glm-130b: An open bilingual pre-trained model. *arXiv preprint arXiv:2210.02414*, 2022.
- [2] Teven Le Scao, Angela Fan, Christopher Akiki, Ellie Pavlick, Suzana Ilić, Daniel Hesslow, Roman Castagné, Alexandra Sasha Luccioni, François Yvon, et al. Bloom: A 176b-parameter open-access multilingual language model. *arXiv preprint arXiv:2211.05100*, 2022.
- [3] Aakanksha Chowdhery, Sharan Narang, Jacob Devlin, Maarten Bosma, Gaurav Mishra, Adam Roberts, Paul Barham, Hyung Won Chung, Charles Sutton, Sebastian Gehrmann, et al. Palm: Scaling language modeling with pathways. *Journal of Machine Learning Research*, 24(240):1–113, 2023.
- [4] Susan Zhang, Stephen Roller, Naman Goyal, Mikel Artetxe, Moya Chen, Shuohui Chen, Christopher Dewan, Mona Diab, Xian Li, Xi Victoria Lin, et al. Opt: Open pre-trained transformer language models, 2022. URL <https://arxiv.org/abs/2205.01068>.
- [5] Manish Gupta and Puneet Agrawal. Compression of deep learning models for text: A survey. *ACM Transactions on Knowledge Discovery from Data (TKDD)*, 16(4):1–55, 2022.
- [6] Mengzhou Xia, Zexuan Zhong, and Danqi Chen. Structured pruning learns compact and accurate models. *arXiv preprint arXiv:2204.00408*, 2022.
- [7] Chaofan Tao, Lu Hou, Haoli Bai, Jiansheng Wei, Xin Jiang, Qun Liu, Ping Luo, and Ngai Wong. Structured pruning for efficient generative pre-trained language models. In *Findings of the Association for Computational Linguistics: ACL 2023*, pages 10880–10895, 2023.
- [8] James O’Neill. An overview of neural network compression. *arXiv preprint arXiv:2006.03669*, 2020.
- [9] Zhiqing Sun, Hongkun Yu, Xiaodan Song, Renjie Liu, Yiming Yang, and Denny Zhou. Mobilebert: a compact task-agnostic bert for resource-limited devices. *arXiv preprint arXiv:2004.02984*, 2020.
- [10] Xiaoqi Jiao, Yichun Yin, Lifeng Shang, Xin Jiang, Xiao Chen, Linlin Li, Fang Wang, and Qun Liu. Tinybert: Distilling bert for natural language understanding. *arXiv preprint arXiv:1909.10351*, 2019.
- [11] Yann LeCun, John Denker, and Sara Solla. Optimal brain damage. *Advances in neural information processing systems*, 2, 1989.
- [12] Babak Hassibi, David G Stork, and Gregory J Wolff. Optimal brain surgeon and general network pruning. In *IEEE international conference on neural networks*, pages 293–299. IEEE, 1993.
- [13] Woosuk Kwon, Sehoon Kim, Michael W Mahoney, Joseph Hassoun, Kurt Keutzer, and Amir Gholami. A fast post-training pruning framework for transformers. *Advances in Neural Information Processing Systems*, 35:24101–24116, 2022.
- [14] Yongqi An, Xu Zhao, Tao Yu, Ming Tang, and Jinqiao Wang. Fluctuation-based adaptive structured pruning for large language models. *arXiv preprint arXiv:2312.11983*, 2023.
- [15] Azade Nova, Hanjun Dai, and Dale Schuurmans. Gradient-free structured pruning with unlabeled data. *arXiv preprint arXiv:2303.04185*, 2023.
- [16] Hao Li, Asim Kadav, Igor Durdanovic, Hanan Samet, and Hans Peter Graf. Pruning filters for efficient convnets, 2017.
- [17] Namhoon Lee, Thalaiyasingam Ajanthan, and Philip HS Torr. Snip: Single-shot network pruning based on connection sensitivity. *arXiv preprint arXiv:1810.02340*, 2018.
- [18] Ashish Vaswani, Noam Shazeer, Niki Parmar, Jakob Uszkoreit, Llion Jones, Aidan N Gomez, Łukasz Kaiser, and Illia Polosukhin. Attention is all you need. *Advances in neural information processing systems*, 30, 2017.

- [19] Trevor Gale, Erich Elsen, and Sara Hooker. The state of sparsity in deep neural networks. *arXiv preprint arXiv:1902.09574*, 2019.
- [20] Mingjie Sun, Zhuang Liu, Anna Bair, and J Zico Kolter. A simple and effective pruning approach for large language models. *arXiv preprint arXiv:2306.11695*, 2023.
- [21] Elias Frantar and Dan Alistarh. Sparsegpt: Massive language models can be accurately pruned in one-shot. In *International Conference on Machine Learning*, pages 10323–10337. PMLR, 2023.
- [22] Yang He and Lingao Xiao. Structured pruning for deep convolutional neural networks: A survey. *arXiv preprint arXiv:2303.00566*, 2023.
- [23] Angela Fan, Edouard Grave, and Armand Joulin. Reducing transformer depth on demand with structured dropout. *arXiv preprint arXiv:1909.11556*, 2019.
- [24] Elena Voita, David Talbot, Fedor Moiseev, Rico Sennrich, and Ivan Titov. Analyzing multi-head self-attention: Specialized heads do the heavy lifting, the rest can be pruned. *arXiv preprint arXiv:1905.09418*, 2019.
- [25] Siqi Sun, Yu Cheng, Zhe Gan, and Jingjing Liu. Patient knowledge distillation for bert model compression. *arXiv preprint arXiv:1908.09355*, 2019.
- [26] François Lagunas, Ella Charlaix, Victor Sanh, and Alexander M Rush. Block pruning for faster transformers. *arXiv preprint arXiv:2109.04838*, 2021.
- [27] Song Han, Huizi Mao, and William J Dally. Deep compression: Compressing deep neural networks with pruning, trained quantization and huffman coding. *arXiv preprint arXiv:1510.00149*, 2015.
- [28] Eldar Kurtic, Daniel Campos, Tuan Nguyen, Elias Frantar, Mark Kurtz, Benjamin Fineran, Michael Goin, and Dan Alistarh. The optimal bert surgeon: Scalable and accurate second-order pruning for large language models. *arXiv preprint arXiv:2203.07259*, 2022.
- [29] Tom Brown, Benjamin Mann, Nick Ryder, Melanie Subbiah, Jared D Kaplan, Prafulla Dhariwal, Arvind Neelakantan, Pranav Shyam, Girish Sastry, Amanda Askell, et al. Language models are few-shot learners. *Advances in neural information processing systems*, 33:1877–1901, 2020.
- [30] Jared Kaplan, Sam McCandlish, Tom Henighan, Tom B Brown, Benjamin Chess, Rewon Child, Scott Gray, Alec Radford, Jeffrey Wu, and Dario Amodei. Scaling laws for neural language models. *arXiv preprint arXiv:2001.08361*, 2020.
- [31] Susan Zhang, Stephen Roller, Naman Goyal, Mikel Artetxe, Moya Chen, Shuohui Chen, Christopher Dewan, Mona Diab, Xian Li, Xi Victoria Lin, et al. Opt: Open pre-trained transformer language models. *arXiv preprint arXiv:2205.01068*, 2022.
- [32] Tim Dettmers, Mike Lewis, Younes Belkada, and Luke Zettlemoyer. Llm. int8 (): 8-bit matrix multiplication for transformers at scale. *arXiv preprint arXiv:2208.07339*, 2022.
- [33] Elias Frantar, Saleh Ashkboos, Torsten Hoefler, and Dan Alistarh. Gptq: Accurate post-training quantization for generative pre-trained transformers. *arXiv preprint arXiv:2210.17323*, 2022.
- [34] Yuhang Li, Ruihao Gong, Xu Tan, Yang Yang, Peng Hu, Qi Zhang, Fengwei Yu, Wei Wang, and Shi Gu. Brecq: Pushing the limit of post-training quantization by block reconstruction. *arXiv preprint arXiv:2102.05426*, 2021.
- [35] Seungcheol Park, Hojun Choi, and U Kang. Knowledge-preserving pruning for pre-trained language models without retraining. *arXiv preprint arXiv:2308.03449*, 2023.
- [36] Jacob Devlin, Ming-Wei Chang, Kenton Lee, and Kristina Toutanova. BERT: Pre-training of deep bidirectional transformers for language understanding. *arXiv preprint arXiv:1810.04805*, 2018.
- [37] Hugo Touvron, Thibaut Lavril, Gautier Izacard, Xavier Martinet, Marie-Anne Lachaux, Timothée Lacroix, Baptiste Rozière, Naman Goyal, Eric Hambro, Faisal Azhar, et al. Llama: Open and efficient foundation language models. *arXiv preprint arXiv:2302.13971*, 2023.
- [38] Alex Wang, Amanpreet Singh, Julian Michael, Felix Hill, Omer Levy, and Samuel R Bowman. GLUE: A multi-task benchmark and analysis platform for natural language understanding. *arXiv preprint arXiv:1804.07461*, 2018.
- [39] Pranav Rajpurkar, Jian Zhang, Konstantin Lopyrev, and Percy Liang. SQuAD: 100,000+ questions for machine comprehension of text. *arXiv preprint arXiv:1606.05250*, 2016.

- [40] Pranav Rajpurkar, Robin Jia, and Percy Liang. Know what you don't know: Unanswerable questions for SQuAD. *arXiv preprint arXiv:1806.03822*, 2018.
- [41] Stephen Merity, Caiming Xiong, James Bradbury, and Richard Socher. Pointer sentinel mixture models. *arXiv preprint arXiv:1609.07843*, 2016.
- [42] Christopher Clark, Kenton Lee, Ming-Wei Chang, Tom Kwiatkowski, Michael Collins, and Kristina Toutanova. Boolq: Exploring the surprising difficulty of natural yes/no questions. *arXiv preprint arXiv:1905.10044*, 2019.
- [43] Yonatan Bisk, Rowan Zellers, Jianfeng Gao, Yejin Choi, et al. PIQA: Reasoning about physical commonsense in natural language. In *Proceedings of the AAAI conference on artificial intelligence*, volume 34, pages 7432–7439, 2020.
- [44] Rowan Zellers, Ari Holtzman, Yonatan Bisk, Ali Farhadi, and Yejin Choi. Hellaswag: Can a machine really finish your sentence? *arXiv preprint arXiv:1905.07830*, 2019.
- [45] Keisuke Sakaguchi, Ronan Le Bras, Chandra Bhagavatula, and Yejin Choi. Winogrande: An adversarial winograd schema challenge at scale. *Communications of the ACM*, 64(9):99–106, 2021.
- [46] Peter Clark, Isaac Cowhey, Oren Etzioni, Tushar Khot, Ashish Sabharwal, Carissa Schoenick, and Oyvind Tafjord. Think you have solved question answering? try arc, the ai2 reasoning challenge. *arXiv preprint arXiv:1803.05457*, 2018.
- [47] Todor Mihaylov, Peter Clark, Tushar Khot, and Ashish Sabharwal. Can a suit of armor conduct electricity? a new dataset for open book question answering. *arXiv preprint arXiv:1809.02789*, 2018.
- [48] Xinyin Ma, Gongfan Fang, and Xinchao Wang. Llm-pruner: On the structural pruning of large language models. *arXiv preprint arXiv:2305.11627*, 2023.
- [49] Adam Paszke, Sam Gross, Francisco Massa, Adam Lerer, James Bradbury, Gregory Chanan, Trevor Killeen, Zeming Lin, Natalia Gimelshein, Luca Antiga, et al. Pytorch: An imperative style, high-performance deep learning library. *Advances in neural information processing systems*, 32, 2019.
- [50] Thomas Wolf, Lysandre Debut, Victor Sanh, Julien Chaumond, Clement Delangue, Anthony Moi, Pierric Cistac, Tim Rault, Rémi Louf, Morgan Funtowicz, et al. Transformers: State-of-the-art natural language processing. In *Proceedings of the 2020 conference on empirical methods in natural language processing: system demonstrations*, pages 38–45, 2020.
- [51] Adina Williams, Nikita Nangia, and Samuel R Bowman. A broad-coverage challenge corpus for sentence understanding through inference. *arXiv preprint arXiv:1704.05426*, 2017.
- [52] Thierry Tambe, Coleman Hooper, Lillian Pentecost, Tianyu Jia, En-Yu Yang, Marco Donato, Victor Sanh, Paul Whatmough, Alexander M Rush, David Brooks, et al. Edgebert: Sentence-level energy optimizations for latency-aware multi-task nlp inference. In *MICRO-54: 54th Annual IEEE/ACM International Symposium on Microarchitecture*, pages 830–844, 2021.
- [53] Hector Levesque, Ernest Davis, and Leora Morgenstern. The winograd schema challenge. In *Thirteenth international conference on the principles of knowledge representation and reasoning*, 2012.
- [54] Ido Dagan, Oren Glickman, and Bernardo Magnini. The pascal recognising textual entailment challenge. In *Machine learning challenges workshop*, pages 177–190. Springer, 2005.
- [55] R Bar Haim, Ido Dagan, Bill Dolan, Lisa Ferro, Danilo Giampiccolo, Bernardo Magnini, and Idan Szpektor. The second pascal recognising textual entailment challenge. In *Proceedings of the Second PASCAL Challenges Workshop on Recognising Textual Entailment*, volume 7, pages 785–794, 2006.
- [56] Danilo Giampiccolo, Bernardo Magnini, Ido Dagan, and William B Dolan. The third pascal recognizing textual entailment challenge. In *Proceedings of the ACL-PASCAL workshop on textual entailment and paraphrasing*, pages 1–9, 2007.
- [57] Luisa Bentivogli, Peter Clark, Ido Dagan, and Danilo Giampiccolo. The fifth pascal recognizing textual entailment challenge. *TAC*, 7(8):1, 2009.

- [58] Richard Socher, Alex Perelygin, Jean Wu, Jason Chuang, Christopher D Manning, Andrew Y Ng, and Christopher Potts. Recursive deep models for semantic compositionality over a sentiment treebank. In *Proceedings of the 2013 conference on empirical methods in natural language processing*, pages 1631–1642, 2013.
- [59] Alex Warstadt, Amanpreet Singh, and Samuel R Bowman. Neural network acceptability judgments. *Transactions of the Association for Computational Linguistics*, 7:625–641, 2019.
- [60] Iyer Shankar, Dandekar Nikhil, and Csernai Kornél. First quora dataset release: question pairs. URL <https://www.quora.com/q/quoradata/First-Quora-Dataset-ReleaseQuestion-Pairs>, 2017.
- [61] Bill Dolan and Chris Brockett. Automatically constructing a corpus of sentential paraphrases. In *Third International Workshop on Paraphrasing (IWP2005)*, 2005.
- [62] Daniel Cer, Mona Diab, Eneko Agirre, Inigo Lopez-Gazpio, and Lucia Specia. Semeval-2017 task 1: Semantic textual similarity-multilingual and cross-lingual focused evaluation. *arXiv preprint arXiv:1708.00055*, 2017.
- [63] Mitchell Marcus, Beatrice Santorini, and Mary Ann Marcinkiewicz. Building a large annotated corpus of english: The penn treebank. 1993.
- [64] Rohan Taori, Ishaan Gulrajani, Tianyi Zhang, Yann Dubois, Xuechen Li, Carlos Guestrin, Percy Liang, and Tatsunori B. Hashimoto. Stanford alpaca: An instruction-following llama model. https://github.com/tatsu-lab/stanford_alpaca, 2023.
- [65] Wei-Lin Chiang, Zhuohan Li, Zi Lin, Ying Sheng, Zhanghao Wu, Hao Zhang, Lianmin Zheng, Siyuan Zhuang, Yonghao Zhuang, Joseph E. Gonzalez, Ion Stoica, and Eric P. Xing. Vicuna: An open-source chatbot impressing gpt-4 with 90%* chatgpt quality, March 2023.

A Implementation Algorithm of LIAR

The detailed steps of our method are outlined in Algorithm 1. The inputs to LIAR encompass the pre-trained language model \mathcal{M} with L attention and FFN layers, each of which contains weight \mathbf{W}^ℓ , bias \mathbf{B}^ℓ and mask variables \mathbf{M}^ℓ . We conduct the reconstruction based on the calibration dataset \mathcal{D} , and return a well-pruned and -recovered model \mathcal{S} .

Our approach decomposes the reconstruction problem for the model \mathcal{M} into layer-wise subproblems. Specifically, we first collect the hidden input for the first layer, then iteratively solve the subproblem and derive the input for the next one. For each subproblem, we first split the input and weight into the unmasked and masked ones respectively based on the mask variables. Building on this, we calculate the mean value for the input to derive the stable pattern given varying samples, and then estimate the transformation matrices for the masked input and weight by solving the least-square problem. Based on the estimated correlations between the pruned and preserved components, the weight and bias are updated accordingly.

Algorithm 1 Linear Interpolation-based Adaptive Reconstruction (LIAR) Framework.

Input: Pre-trained language model \mathcal{M} with L layers. Mask variables \mathbf{M}^ℓ , weight \mathbf{W}^ℓ , and bias \mathbf{B}^ℓ for layer ℓ . Calibration dataset \mathcal{D} .

- 1: Initialize model \mathcal{S} : $\mathcal{S} \leftarrow \mathcal{M}$.
- 2: **for** sample in \mathcal{D} **do**
- 3: Collect hidden input \mathbf{X}^ℓ for $\ell = 1$ of model \mathcal{S} .
- 4: **for** $\ell \leftarrow 1$ to L **do**
- 5: Split \mathbf{X}^ℓ and \mathbf{W}^ℓ into \mathbf{X}_u^ℓ , \mathbf{X}_m^ℓ , \mathbf{W}_u^ℓ , and \mathbf{W}_m^ℓ respectively based on the mask \mathbf{M}^ℓ .
- 6: Calculate the mean value of \mathbf{X}^ℓ : $\bar{\mathbf{X}}^\ell = \frac{1}{NT} \sum_{i=1}^N \sum_{j=1}^T \mathbf{X}_{i,j,\cdot}^\ell$.
- 7: Estimate \mathbf{Q}^ℓ for the input: $\mathbf{Q}^\ell = \arg \min_{\mathbf{Q}^\ell} \left\| \mathbf{X}_m^\ell - \left(\mathbf{X}_u^\ell \mathbf{Q}^\ell + \bar{\mathbf{X}}_m^\ell \right) \right\|_2^2$.
- 8: Estimate the transformation matrix \mathbf{P}^ℓ for the weight: $\mathbf{P}^\ell = \arg \min_{\mathbf{P}^\ell} \left\| \mathbf{W}_m^\ell - \mathbf{P}^\ell \mathbf{W}_u^\ell \right\|_2^2$.
- 9: Update the weight: $\mathbf{W}^\ell \leftarrow (\mathbf{I} + \mathbf{Q}^\ell \mathbf{P}^\ell) \mathbf{W}_u^\ell$.
- 10: Update the bias: $\mathbf{B}^\ell \leftarrow \bar{\mathbf{X}}_m^\ell \mathbf{W}_m^\ell + \mathbf{B}^\ell$.
- 11: Collect hidden input $\mathbf{X}^{\ell+1}$ based on the updated weight \mathbf{W}^ℓ and bias \mathbf{B}^ℓ .

Output: Pruned and recovered model \mathcal{S}

B Experimental Setup

B.1 Models

We introduce two categorized models in our experiments: BERT_{BASE} [36] and LLaMA family models [37]. BERT_{BASE} of 0.1B parameters is an encoder-based model, which is stacked by 12 Transformer layers, each of which has 12 attention heads and 3072 FFN neurons, and the embedding dimension is 768. LLaMA is a set of decoder-based large language models open-sourced by Meta, mainly including LLaMA-7B/13B/30B/65B, and limited by the computing resources, we only choose the 7B, 13B, and 30B sizes to conduct experiments. Take the LLaMA-7B as an example, it consists of 32 decoder layers, whose embedding size is 4096, and the number of attention heads and FFN neurons are 32 and 11008 respectively.

B.2 Tasks

GLUE Benchmark. The GLUE (General Language Understanding Evaluation) benchmark is a collection of datasets for evaluating the performance of models across a diverse set of existing natural language understanding tasks. GLUE consists of 3 categorized sequence classification tasks: 1) Natural language inference (MNLI [51], QNLI [52], WNLI [53], RTE [54, 55, 56, 57] with 393K, 105K, 0.6K and 2.5 K training samples), 2) Single-sentence classification (SST-2 [58], CoLA [59] with 67K and 8.5K training examples), and 3) Similarity and paraphrase (QQP [60], MRPC [61],

STS-B [62] with 364K, 3.7K and 7K training samples respectively). We exclude the WNLI, RTE, and CoLA tasks due to their unstable performance. For the other tasks, we prune the model by using the training set of each dataset for different tasks and report the Accuracy on the development sets except for the STS-B task, for which we report the Spearman Correlation.

SQuAD. The SQuAD (Stanford Question Answering Dataset) is a reading comprehension dataset for the question-answering task, which is categorized into 2 versions: SQuAD_{1.1} [39] and SQuAD_{2.0} [40], each of which contains 88K and 130K training examples. To be specific, SQuAD_{2.0} is an extension of SQuAD_{1.1} by including unanswerable questions about the same paragraphs whose answers are not stated in the given contexts. We report the F1 score for SQuAD tasks.

WikiText. The WikiText corpus is a language modeling benchmark dataset, which is a hundred times larger than the previous Penn Treebank [63]. This corpus is available in two data sizes: WikiText-2 and WikiText-103, which have 2K and 103K training samples respectively. Both datasets use the same articles for validation and testing. We follow [14] to conduct pruning on the WikiText-2 training set and report the perplexity metric for the test set, which gauges a model’s predictive accuracy.

Common Sense Reasoning Benchmarks. We conduct experiments on seven pivotal common sense benchmarks to evaluate the model’s zero-shot performance: BoolQ [42], PIQA [43], HellaSwag [44], WinoGrande [45], ARC-easy [46], ARC-challenge [47] and OpenbookQA [47]. We conduct the reconstruction on the Alpaca dataset [64] and report both the accuracy of each benchmark and the overall average accuracy.

B.3 Baselines

Retraining-free Pruning Methods. To our best knowledge, [13] is the first post-training pruning framework for transformers, which proposed Mask Search and Mask Rearrangement to measure the importance of attention heads and neurons based on the Fisher information, and Mask Tuning to recover its accuracy. KCM (Kernelized Convex Masking) [15] proposed two ranking techniques to estimate the importance of individual neurons: Representative Ranking (R2) and Data-Driven (D2). It is noticed that KCM only prunes the neurons, and it brings about significant performance degradation under large compression rates as shown in Table 2. While previous studies concentrate on BERT-based models, FLAP (Fluctuation-based Adaptive Structured Pruning) focuses on decoder-based models such as the LLaMA model family and the Vicuna-7B model [65]. FLAP prunes the most stationary heads and neurons and utilizes the average value of the pruned components as a bias to compensate for the output error.

Existing Reconstruction Algorithms. Naive pruning means direct pruning without any retraining or reconstruction, which represents the efficacy of the pruning criteria to some extent and serves as a baseline for different reconstruction strategies. Mask Tuning is a reconstruction technique proposed by [13], which rescales the nonzero mask values to any real values instead of being restricted to 1 by layer-wise reconstruction via linear least squares. This technique is also utilized by KCM. Bias Compensation is proposed by [14], which operates by calculating the average value of the attention or FFN output matrix and multiplying it with the pruned weight to obtain a bias to compensate for the distorted output.

B.4 Pruning Criteria.

We introduce two pruning metrics that require retraining to avoid hurting the performance: Weight Magnitude and SNIP.

Weight Magnitude. Weight Magnitude [16] is a conventional pruning criterion based on the magnitude of filters, which utilizes the zero-order information of the weight and prunes the filters with small magnitudes. The importance score for k -th filter $\mathcal{F}_k \in \mathbb{R}^{n_i \times l \times l}$ with n_i input channels and kernel width l is calculated as

$$s_k = \sum \|\mathcal{F}_k\|_1. \tag{10}$$

SNIP. SNIP (Single-shot Network Pruning) [17] is a simple but effective technique that measures the sensitivity of the connections and allows us to identify and prune the redundant connections in a single step. To be specific, given the dataset \mathcal{D} and weight \mathbf{w} with m connections, the effect of removing connection c_k is first calculated by

$$\Delta L_k(\mathbf{w}; \mathcal{D}) \approx g_k(\mathbf{w}; \mathcal{D}) = \left. \frac{\partial L(\mathbf{c} \odot \mathbf{w}; \mathcal{D})}{\partial c_k} \right|_{\mathbf{c}=\mathbf{1}}, \quad (11)$$

where $\mathbf{c} \in \{0, 1\}^m$ are indicator variables representing the connectivity of \mathbf{w} . The magnitude of the derivatives g_k is taken as the saliency criterion and normalized to obtain the importance score:

$$s_k = \frac{|g_k(\mathbf{w}; \mathcal{D})|}{\sum_{j=1}^m |g_j(\mathbf{w}; \mathcal{D})|}. \quad (12)$$

The connections with the least importance scores are removed directly accordingly.

C Detailed Implementation

C.1 Tasks & Datasets

We download the datasets from the Huggingface repositories on GLUE, SQuAD, WikiText, BoolQ, PIQA, HellaSwag, WinoGrande, ARC, and OBQA benchmarks. We employ the EleutherAI LM Harness³, a public evaluation benchmark, to evaluate the zero-shot performance on the seven common sense reasoning benchmarks.

C.2 Models

We download the BERT_{BASE} model⁴ and LLaMA-7B model⁵ from the Huggingface repository. To obtain the task-specific BERT model, we finetune the pre-trained BERT_{BASE} to the downstream tasks following a standard training recipe.

C.3 Implementation for Retraining-free Pruning Methods

We utilize the released code by authors⁶ to implement [13]. We use damp=1 for LSMR solver⁷ in CuPy and an acceptable range of tuned variables as $[-10, 10]$ as the paper described. All of the experimental settings are kept to default. As for the KCM, we reimplement it since there is no public implementation of authors. We use width $\sigma = 1$ for the Gaussian kernel and convergence rate $\alpha = 0.01$ in the paper [15]. We use Z-score normalization for normalizing the D2 scores. Towards the FLAP, we follow of implementation of authors⁸.

C.4 Implementation for Reconstruction Algorithms

As part of [13] and FLAP, we implement Mask Tuning and Bias Compensation following the released code and fix the samples to be 2048, 1024, and 1024 for Mask Tuning, Bias Compensation, and LIAR respectively.

C.5 Implementation for Pruning Criteria

Weight Magnitude. As the weight magnitude-based pruning method is originally designed for convolutional kernels, which is not well-suited for pruning FFN neurons of the transformer block, we modify the metric to align with the characteristics of the transformer layer. We also utilize the

³<https://github.com/EleutherAI/lm-evaluation-harness>

⁴<https://huggingface.co/bert-base-uncased>

⁵<https://huggingface.co/linhvu/decapoda-research-llama-7b-hf>

⁶<https://github.com/WoosukKwon/retraining-free-pruning>

⁷[cupyx.scipy.sparse.linalg.lsmr](https://pypi.org/project/cupyx-scipy-sparse-linalg-lsmr/)

⁸<https://github.com/CASIA-IVA-Lab/FLAP>

ℓ_2 -error as it yields higher accuracy according to our experimental results, and the resulting accuracy is similar to the implementation in [15]. The adapted metric takes the following term:

$$s_k = \sum_{i=1}^{C_{out}} \|\mathbf{W}_{k,i}\|_2^2, \quad (13)$$

where $\mathbf{W} \in \mathbb{R}^{C_{in} \times C_{out}}$ is the output matrix of the FFN layers.

SNIP. The size of dataset \mathcal{D} for pruning is fixed to 5K for all tasks, which yields fairly stable performance according to our empirical analysis.

C.6 Other Details

We implement our framework and the baselines with Pytorch [49] and Huggingface Transformers [50] libraries. To save the memory consumption, we load the model onto the GPU in 16-bit floating-point format when pruning the LLaMA models.

C.7 Generalization to Pruning Modules on Other Tasks

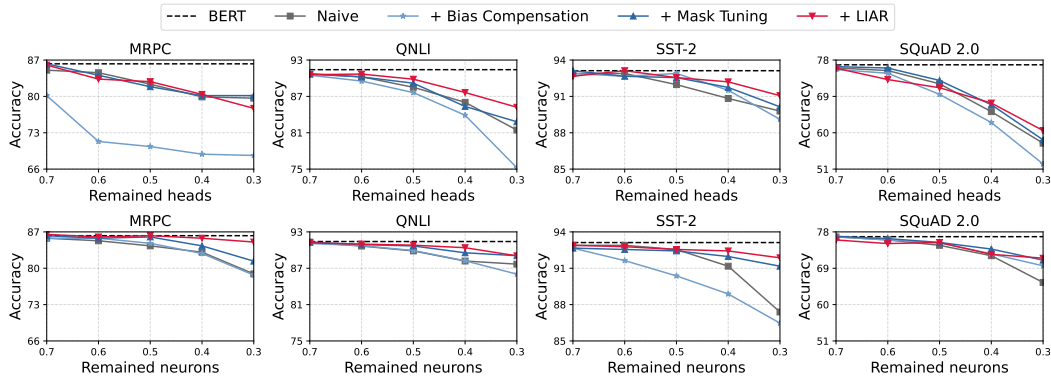


Figure 7: Performance comparison of the $BERT_{BASE}$ on MRPC, QNLI, SST-2 and SQuAD_{2.0} tasks by pruning attention heads (**upper**) and FFN neurons (**lower**) with different reconstruction strategies.

Figure 7 demonstrates the performance comparison on MRPC, QNLI, SST-2, and SQuAD_{2.0} tasks by removing attention heads and FFN neurons respectively based on the importance score derived by [13]. Our approach recovers the pruned output and achieves higher accuracy on most occasions.

C.8 Generalization to Pruning Criteria on Other Tasks

Figure 8 shows the effectiveness of our method for two retraining-based pruning criteria: Weight Magnitude and SNIP. It is obvious that LIAR attains the most consistent and significant performance improvements across both pruning metrics and nearly all the tasks and pruning ratios.

D Limitations

Although this study brings significant performance enhancement for retraining-free pruning, it still faces two important potential limitations for future research directions. (1) Firstly, as our method utilizes calibration samples, it shares a similar and common issue with all of the data-driven approaches, which will encounter an overfitting problem with limited data. Most works choose to facilitate it by feeding numerous samples to guarantee stable performance (e.g., retraining-based methods) while our approach has a rather lower requirement for the dataset size compared to conventional data-driven approaches as demonstrated in Figure 6 and thus to be more efficient. (2) Secondly, as our method is applicable to varied pruning metrics and does not involve determining the network architecture, the regained performance is dependent on the quality of the pruning criteria. In other words, whether a pruned model can be reconstructed through LIAR is based on whether

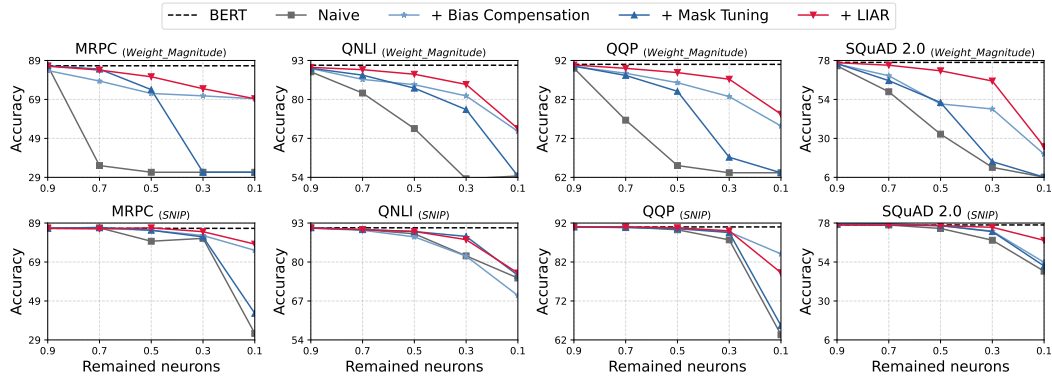


Figure 8: Performance comparison of the $BERT_{BASE}$ pruned by Weight Magnitude-based (**upper** lines) and SNIP (**lower** lines) criteria on the MRPC, QNLI, QQP and SQuAD_{2.0} tasks respectively, in which we only prune the FFN neurons to avoid to introduce the architecture search problem.

the pruned parts are recoverable. Or, to put it another way, we think this characteristic may not be a drawback, but exactly makes our method a powerful validation tool to evaluate the quality of a specific pruning criterion.

E Broader Impacts

In this paper, we introduce a method that stands out for its computational efficiency and the elimination of the need for retraining, while still delivering enhanced performance metrics. Our innovation paves the way for rapid compression and deployment processes for large language models, making it an invaluable resource for scenarios constrained by limited computational capabilities. Through comprehensive analysis, we have yet to identify any adverse effects associated with our proposed method, underscoring its potential for widespread application without negative repercussions.